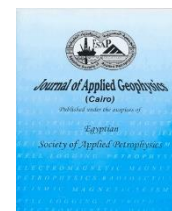




ISSN: 1687-1251

Egyptian Society of Applied Petrophysics

Journal of Applied Geophysics (Cairo)

Journal home page: <https://jag.journals.ekb.eg/>

Original Article

Petrophysical Evaluation of Khatatba Formation in El-Obaiyed Area, Northern Western Desert, Egypt

Mohammad Monir Kamal Mahmoud^{1*}, Ahmed Sayed Abu El-Ata¹, Amir Maher Lala¹

¹ Department of Geophysics, Faculty of Science, Ain Shams University, Cairo, Egypt.

ARTICLE INFO

Keywords:

Petrophysics,
El-Obaiyed Area,
North-Western Desert,
Egypt

El-Obaiyed area is part of the north-Western Desert gas producing fields in Egypt. It is approximately 50 km to the south of the Mediterranean coast and about 450 km west northwest of Cairo. The Obaiyed Field lies on the western flank of the Matruh basin. The study employs geological and petrophysical data. The objective of this work is to delineate the hydrocarbon-bearing zones and predict reservoir fluid behavior. The study employs a multidisciplinary approach, combining geological and petrophysical data, to characterize the rock properties and fluid behavior within the subsurface formations. Well log data are integrated together, to build a comprehensive understanding of the reservoir properties. The objective of this work is to delineate the hydrocarbon-bearing zones and to predict the reservoir fluid behavior. This study results are based on the geological and geophysical data, provided by Badr Petroleum Company (BAPETCO), upon the approval of the Egyptian General Petroleum Corporation (EGPC). In addition, the well log data of four wells (D15, D19, OBA D-32 and OBA D-35) are distributed through the study area. The results from this study identified the potential reservoirs accumulating primarily in Lower Safa Member and secondary gas-bearing Upper Safa Member, where evaluation showed an average gross thickness of 100 m in Upper Safa with porosity average range 3-7% and a gross thickness of 93 m in Lower Safa with an average porosity range 6-12%, as well as Kabrit formation which came out with good gas-bearing net thickness in well OBA D-35. The Lower Safa Member is subdivided into multiple units, composed of sand and shale intercalations with thickness thinning southwards. Higher effective porosity and permeability values were noticed for the sand, while the Lower values are found for the shale. Furthermore, the stratigraphic correlation and the GDT values of the reservoir negates the continuity between the studied wells, with the possibility of several compartments in the area.

* Corresponding author at: Geophysics Department, Faculty of Science, Ain Shams university, Cairo, Egypt.
gmonir95@gmail.com

1- Introduction

1.1 General View

El-Obaiyed gas/oil field is one of the largest gas producing fields located at the extreme north western corner of the Western Desert of Egypt (Fig. 1). It lies between latitudes 31° 02` and 31° 12` N and longitudes 26° 34` and 26° 45` E approximately 50 km to the south of the Mediterranean coast and about 450 km west northwest of Cairo. El-Obaiyed field is located within Matruh Basin, which is an intracratonic passive rift basin, active mainly during Jurassic/early Cretaceous. The Lower Safa Member of the Khatatba Formation is responsible for the majority of the total hydrocarbon output. Production in the field began in late 1999, with tight Middle Jurassic sandstones at a depth of around 4,000 meters. Because El-Obaiyed is a somewhat complicated field with significant permeability distribution errors, linked Gas Initially in-Place computations may not always be accurate. In 1990, many studies indicated that, 90% of oil and 80% of gas expected potentials are yet to be found (EGPC, 1992 and Ghanima 2015). The 20% failure rate of the development wells in the El-Obaiyed field region indicates that despite the drilling of more than 48 wells, there are still substantial subterranean uncertainties in the reservoir quality and its extension (Saad, et al., 2010).

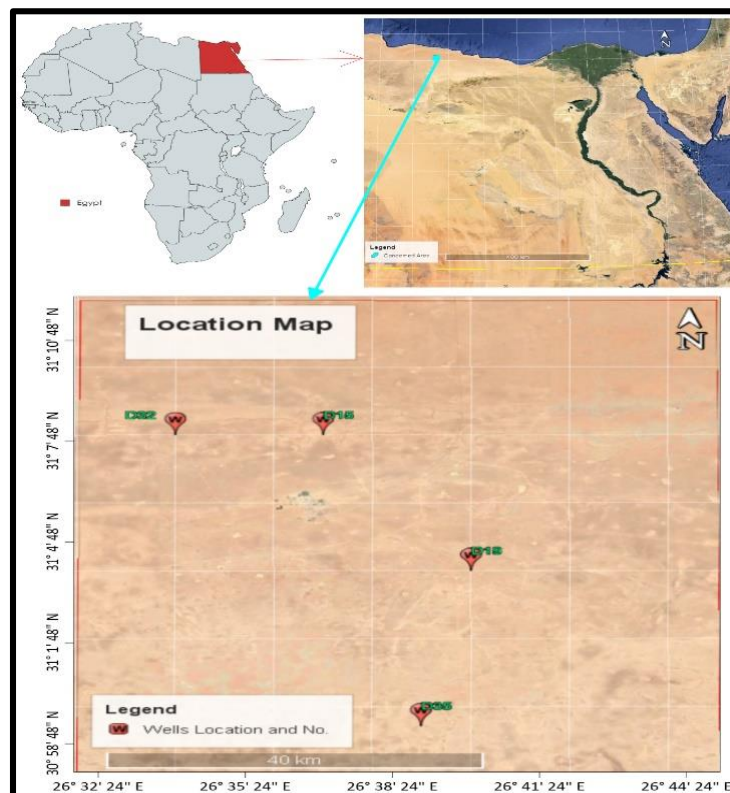


Fig. 1: Concession map of BAPETCO, showing the location of El-Obaiyed field.

1.2 Exploration History of the Western Desert

The Anglo- Egyptian Oil Company drilled the EL Daba-1 well in the northern portion of the Western Desert in 1940, marking the beginning of exploratory operations in Egypt's Western Desert. At the time, there were some oil indicators found in the Eocene rocks (**EGPC, 1992**). The Alamein Field, which produced from the Alamein Dolomite and Alam EL-Bueib Sandstone, was the first oil field discovered in the Western Desert by PHILIPS in 1969. Nearly 80 million barrels of oil were produced from this field up to 1992.

With the discovery of the Salam-3 well in 1985, Phoenix brought life to the Western Desert oil exploration again, finding three pay-zones in the Bahariya, Alam El-Bueib, and Khatatba formations. The oil and gas discoveries from the Khatatba Formation's Jurassic sandstones mark a paradigm shift in this province's exploration methods as they are the first of their kind in the Western Desert. The Western Desert's Mesozoic basins presented intriguing but challenging exploring possibilities. This is a result of the intricate structure past, and structural traps have been the only thing explored (**Dolson, et al., 2001 and Farag 2010**).

An analysis of the petroleum resources in the Western Desert, north of latitude 28°N, was conducted in 1990. It is estimated that 80% of the potential for gas and 90% of the potential for oil remains undiscovered. In order to access these residual hydrocarbon resources, significant work must be done (**EGPC, 1992**).

1.3 Previous studies in the north Western Desert

In this study, an effort was made, to review and evaluate the literatures of the Western Desert, specifically those related to oil and gas exploration. The northern area of the Western Desert is an auspicious oil and gas province and has been the center of interest of geologic studies and operations by many oil companies in comparison to the southern part, where relatively smaller number of studies have been concluded.

The history of geologic studies of the north Western Desert was described in the work of **Abu El Ata (1981) and Hamimi (2020)**. In addition to the history exploration of the north Western Desert oil and gas province collected by **Hagras, et al, (1986)**.

Various studies, concluded by different authors, threw light on the hydrocarbon potentialities and oil companies working on the Western Desert, as they contemplated this tract as a very propitious oil and gas province. Worth mentioning authors, among them were **Robertson Research International (1982), Abu El Naga (1984) and Labib (1985), Hamimi (2020), Bosworth (2021)**.

2. Geologic Setting

About two thirds of Egypt's total land area is made up of the Western Desert. The unstable Egyptian shelf contains the northern part of the Western Desert (**Said, 1962**). Numerous sedimentary intracratonic rift basins are a prominent feature in the northern Western Desert (Fig. 2). The majority of the aforementioned basins were begun in the Late Jurassic–Early Cretaceous (Mesozoic basins) although others, like the Northern and Southern Faghur basins, date back to the Permian (**Guiraud, 1998**). The Western Desert's basins have been impacted by several structural phases, including Jurassic rifting, Cretaceous rifting, and Late Cretaceous-Tertiary inversion. These periods brought with them a dense succession of sediments from the Paleozoic to the Cenozoic (Neogene). The western coastal basins (Matruh, Shoushan, Alamein, and Natrun) span an approximate area of 3800 km² and are situated in the far northwest of the Western Desert (**Hamimi, 2020 and Bosworth, 2021**).

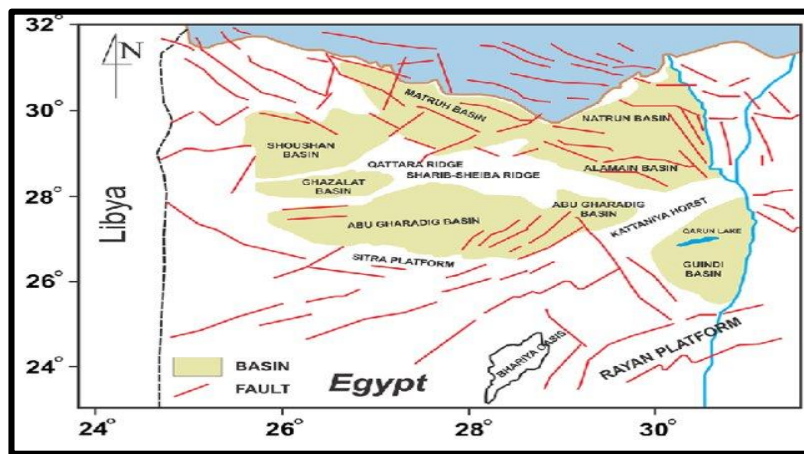


Fig. 2: A map illustrating the major sedimentary basins of the northern Western Desert of Egypt. (after **Haby S. Mohamed et al., 2014**)

The sedimentary cover increases gradually from about 6,000 ft in the south to more than 25,000 ft along the northern coastal basins (**Sultan and Halim, 1988**). The sedimentary section, therein, is divided into three mega-sequences. **Said (1962)**, **Younes (2002)** and **Hamimi (2020)** identified three major clastic megasequences: the middle carbonate megasequence (Cenomanian to Eocene), the upper clastic megasequence (Oligocene to Recent), and the lower clastic megasequence (Cambrian to pre-Cenomanian). The majority of the sedimentary succession, from the Pre-Middle Jurassic to the Recent, is represented in the stratigraphic column of the Matruh basin). Four sedimentary cycles—the Lower to Upper Jurassic, Lower Cretaceous, Upper Cretaceous, and Eocene to Miocene—make up the post-Paleozoic succession in this region (**Sultan and Halim, 1988**). The following lines will provide a brief description of the Mesozoic rock units in the northern Western Desert.

The Mesozoic rock units are the main reservoir and pay zones in all the Western Desert oil fields and are characterized by continental to shallow marine depositional environments all

over the Western Desert, south of Latitude 28° N (Schlumberger, 1984, EGPC, 1992, Hmimi 2020 and Bosworth 2021). The Jurassic and Cretaceous deposits symbolize the Mesozoic section.

Abu El Ata (1981), Hamimi (2020) and Bosworth (2021) delineated different trends of the subsurface regional structural deformations by the geophysical-geological evaluation for the Eastern part of the northern Western Desert, as well as Northern Egypt. The oldest of them is the Meridian System of folds (Precambrian - Early Paleozoic), which has NNW - SSE trend. The second is the Atlas System of folds and fractures (Late Paleozoic - Early Mesozoic), which has NNE - SSW trend. The third is the Syrian Arc system of folds and faults (Middle Mesozoic - Late Mesozoic), which has NE-SW trend. The fourth is the Red Sea system of faults and folds (Early Tertiary), which has NW-SE trend. The fifth is the Mediterranean Sea system of faults (Late Tertiary), which has E-W trend and the sixth is the Aqaba System of faults (Quaternary), which is of N -S trend.

3. Methodology

3.1 Available Data

The available data used in performing the present study include: Wireline logs of four wells (D-15, D-13, D-32 and D-35) which provide Spontaneous potential, Resistivity, Gamma-Ray. Density and Neutron.

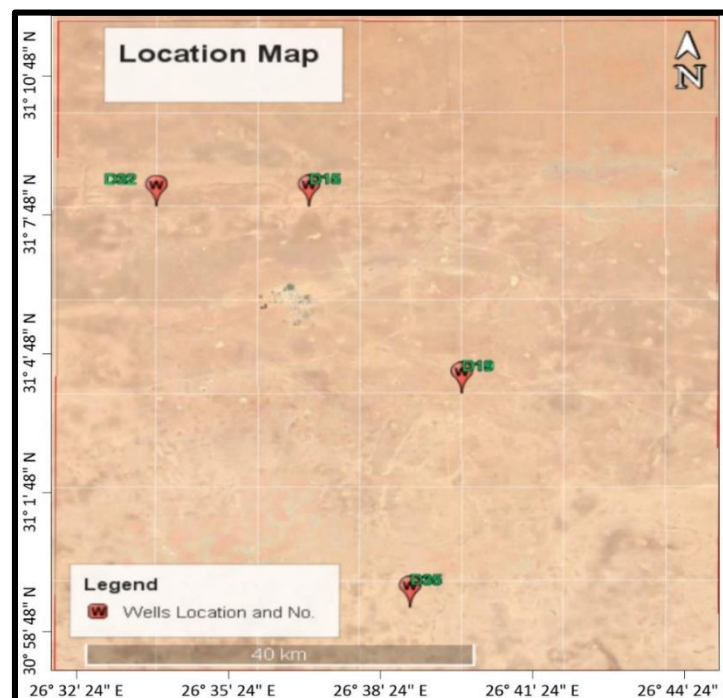


Figure 3: Location of the wells in the study area.

3.1 Petrophysical Evaluation

Formation evaluation includes analyzing the physical properties of rocks, such as porosity, permeability and, saturation, and merging them with the engineering and geological data, to infer the subsurface environments. Formation evaluation is an extremely crucial step in the exploration and development of hydrocarbon reservoirs, as it aids in recognizing the promising drilling locations, estimating the optimal production methods and determining the expected production rates and highest recovery (Ayseth, Mavko, Mukerji and Dvorkin, 2009).

Formation data are acquired, using the wireline logging logs, that is called logging while drilling tools. The data obtained are then combined and analyzed for the following purposes:

- Evaluating the reservoir and assessing the existence of potential hydrocarbon quantities.
- Recognizing any hydrocarbon amount, which might be substantial from an exploration perspective.
- Identifying the productive reservoir characteristics (static and dynamic).
- Establishing the facies correlation and drilling location is by generating the geologic maps.

Determining the Volume of Shale (V_{sh})

Estimating the number of clay minerals in the formation is the first stage in petrophysical investigation. Numerous techniques are employed to ascertain this; a few are covered below. In this stage, the percentages, or quantities of clay minerals in a reservoir are preserved, but neither the kind of clay nor its distribution among reservoirs are. Clay minerals are not likely to be significantly affecting the log responses when the volume of shale (V_{sh}) is less than 15% of the volume of bulk rock.

V_{sh} from Gamma-Ray (Single Indicator)

A linear function of the borehole-corrected gamma ray response may be used to express the volume of shale (V_{sh}):

$$GR=A+B+V_{sh} \dots\dots\dots(1)$$

Since this criterion is typically not satisfied, there is a need to find the V_{sh} using a different technique. This other approach necessitates the ability to compute the Gamma-Ray Index (IGR), and it has been used for this study, as it is one of the most important shale indicators in the evaluation of shaly formations. The main purpose of using the Gamma-Ray Log is to indicate the clay content and lithology (Gibson, 1998 and Gomaa, 2017). To determine the proportion of shale contained in a reservoir, all that must be done is normalize the gamma-ray response.

$$I_{GR} = \frac{GR_{log} - GR_{min}}{GR_{max} - GR_{min}} \dots\dots\dots(2)$$

Gamma-Ray Index (IGR) is the best measure for laminated shales since it is a linear representation of the V_{sh}. In this instance, the ratio that is obtained indicates the proportion of

clay minerals present in the reservoir.

V_{sh} from Neutron-Density Logs

A more popular technique for determining the V_{sh} in a deposit that may contain clay is to combine density log and neutron porosity data as follows: $V_{sh} = \frac{(\Phi_n - \Phi_d)}{(\Phi_{nsh} - \Phi_{dsh})}$ (2)

where:

Φ_n is the neutron porosity in the zone of interest.

Φ_d is the density porosity in the zone of interest.

Φ_{nsh} is the neutron porosity of the adjacent shale zone.

Φ_{dsh} is the density porosity of the adjacent shale zone.

The presence of clays affects both density and neutron values. Neutron and density responses overestimate the impact of kaolinite and chlorite when used to calculate the V_{sh}. Neutron porosities in kaolinite and chlorite are higher than those in montmorillonite and illite (Asquith, 1990).

Effective Porosity from Neutron-Density Combinations

In essence, a formation's hydrogen content is estimated using the neutron logs. An excellent source of porosity data is the combination of the neutron and density logs, particularly in formations with complicated lithology. This technique simultaneously records the neutron and density porosity.

$$\Phi_{n-corrected} = \Phi_n - (V_{cl} \times \Phi_{nsh}) \quad \Phi_{d-corrected} = \Phi_d - (V_{cl} \times \Phi_{dsh}) \dots(3)$$

These values of the neutron and density porosity, adjusted for the presence of clays, are then employed in the equations below to estimate the effective porosity ($\Phi_{effective}$) of the formation of interest.

$$\Phi_{effective} = \left[\frac{(\Phi_{n-corrected})^2 + (\Phi_{d-corrected})^2}{2} \right]^{0.5} \quad \text{for gas} \dots\dots(4)$$

Determining the Water Saturation (S_w)

The effective water saturation simply refers to the percentage of effective porosity occupied by water, whereas the total water saturation (S_{wt}) refers to the percentage of total porosity occupied by water (Asquith, 1990).

Archie's popular equation was established, to estimate the water saturation (S_w) in the un-invaded zone in a formation alongside the borehole from well log parameters. Archie's

$$S_w = \left(\frac{a \times R_w}{R_t \times \phi^m} \right)^{\frac{1}{n}}$$

equation is as follow:(5)

where:

S_w is the water saturation of the uninvaded zone.

A is Archie’s constant.

n is the saturation exponent; it is typically 2.0 but can range from 1.8 to 4.0.

R_w is the formation water resistivity at formation temperature.

Φ is the Porosity.

m is the cementation exponent; it is typically 2.0 but can range from 1.7 to 3.0.

R_t is the true resistivity of the formation, corrected for invasion, borehole, thin bed and other effects.

The water saturation of the flushed zone (S_{xo}) according to Archie equation is as follows:

$$S_{xo} = \left(\frac{a \times R_{mf}}{R_{xo} \times \phi^m} \right)^{\frac{1}{n}} \dots\dots\dots(6)$$

S_{xo} is the water saturation of the flushed zone.

Determining the Hydrocarbon Saturation

Formation true resistivity (R_t) is essential and extremely important for evaluating well logs and to acknowledge the existence of hydrocarbons. R_t is the resistivity of the formation without any drilling fluids in it. Commonly the formation true resistivity holds only water (S_w "water saturation" = 100%) or formation water and hydrocarbons ($S_w < 100\%$). The total percentage of S_w and S_h must equal 100%.

The uninvaded-zone and flushed-zone water saturation are used to determine hydrocarbon saturation. The following formula can be used to determine the hydrocarbon saturation:

$$S_h = 1 - S_w \dots\dots\dots(7)$$

There are two more categories of hydrocarbons: movable and residual oils. The residual hydrocarbon saturation (S_{hr}) may be calculated using the following equation by first calculating the water saturation in the flushed zone:

$$S_{hr} = 1 - S_{xo} \dots\dots\dots(8)$$

Subsequently, we can calculate the moveable oil saturation (S_{hm}) using this equation:

$$S_{hm} = S_h - S_{hr} \dots\dots\dots(9)$$

Reserve Estimation

Reserve estimation of hydrocarbon is the profitable volume of hydrocarbon, that can be withdrawn from a reservoir conducting present techniques. The entire volume of hydrocarbon stored in a reservoir prior to production is defined as original oil-in-place (OOIP) and original gas-in-place (OGIP) (Drake, 1978 and Gomaa, 2017).

The hydrocarbon reserve can be estimated for oil or gas, using the following volumetric equation:

$$IGIP \text{ (Initial Gas in Place)} = 43560 * \phi * (1-S_w) * H * A \dots\dots(10)$$

where:

- IGIP unit is a standard cubic foot (Scf).

- 43560 is the Conversion factor from acre-ft to scf.
- A is the area of the reservoir in acres.
- H is the height/thickness of pay zone (ft.).
- \emptyset is the porosity in decimals.
- S_w is the initial water saturation in fraction.
- B_g is the gas formation volume factor, rcf/scf.

Furthermore, the recoverable hydrocarbon reserves are affected by the accuracy of the reservoir drive mechanism (recovery factor). The primitive equation employed to calculate the recoverable hydrocarbon reserve is:

$$\text{Recoverable oil or gas reserve} = \text{OHIP} * \text{R.F} \quad (11)$$

Where:

R.F. is the Recovery factor.

The volumetric equation technique includes calculation of the reservoir volume through maps and the petrophysical data of drilled wells. Rectifying the subsurface volumes to standard units of volume estimated at the surface condition is crucial in OOIP and IGIP calculations, where a notable volume of gas arises from the oil, due to the reduction of circumambient pressure and temperature, this leads oil at surface to settle in an area smaller than that in the subsurface. On the contrary, gas at surface due to expansion will fill the extra space than it does in the subsurface (**Urayet, 2002 and Ahmed, S. 2019 and**).

4. PETROPHYSICAL EVALUATION RESULTS

In the present work, various wireline tools, such as Gamma-ray logs, Resistivity logs, Porosity tools and Caliper logs are used, to evaluate different rock types and to identify their petrophysical parameters.

The parameters of the potential reservoirs are used to compute the Original Gas-in-Place (OGIP) in the area, by implementing the volumetric equations, that are acquired from the software analysis. These are based on the theoretical equations of the Volume of shale (V_{sh}), Formation water resistivity (R_w), Formation resistivity (R_t), Water saturation (S_w) and Porosity (Φ), as discussed previously.

4.1 Petrophysical QC Logs

It is essential to match the log data with the wireline tools, due to several geologic conditions. Environmental corrections were applied on the log data, to eliminate the environmental errors like the mud cake effect and invasion effect. Multi-Well histogram was used in this study, to check the range of data of each log. (Fig. 4) shows the GR Multi-Well histogram, which validates the data range from 10 to 150 API. The resistivity Multi-Well histogram in (Fig. 5) shows the logarithmic data range from 0.0022 to 2000.0079 ohm.m.

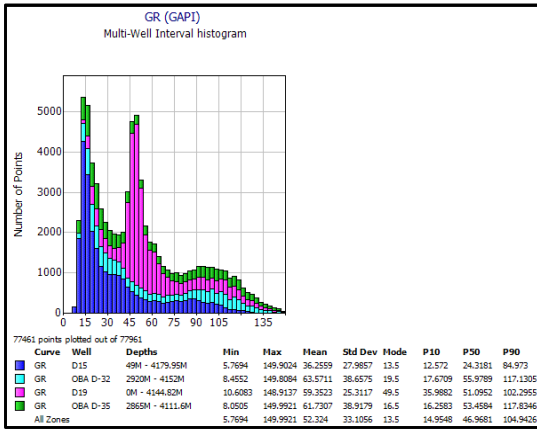


Fig. 4: GR log histogram for the wells D-15, D-19, OBA D-32 and OBA D-35.

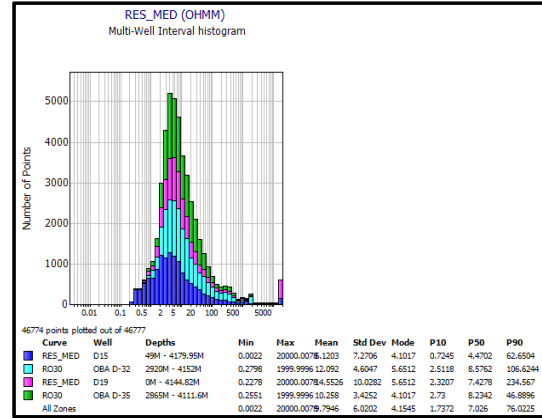


Fig. 5: Resistivity log histogram for the wells D-15, D-19, OBA D-32 and OBA D-35.

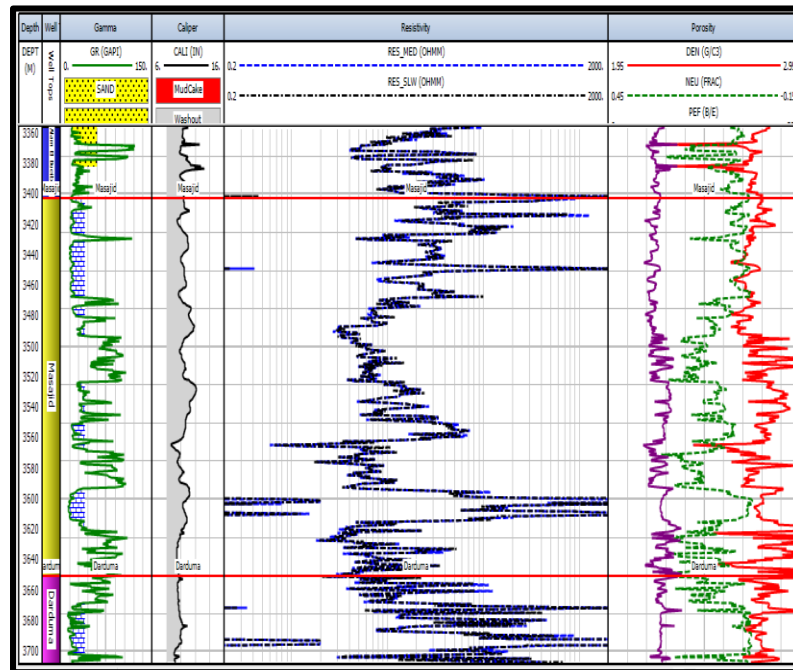


Fig. 6: QC Plot showing the washout, also using the caliper and Bit size log in Alam El-Bueib 1 bottom, Masajid and Darduma formations.

In El Obaiyed area the mud circulations losses were encountered during the drilling process, which can be clearly detected, using the caliper log, particularly in Jurassic carbonate formations (Limestone), like Masajid, Darduma and in Cretaceous clastic (Sandstone) formation Alam El Bueib D1 bottom as well as shown in the below (Fig. 6).

4.2 Reservoir Parameters and Results

Conventional logs were used for D-15, D-19, OBA D-32 and OBA D-35 wells, to obtain the effective porosity, volume of shale and water saturation values through calculations. Input

parameters and Cutt-off values were extracted from **BAPETCO** Internal reports production data. Figures (7, 8, 9 and 10) show the calculation of porosity and water saturation for the potential zones in D-15, D-19, OBA D-32 and OBA D-35 wells respectively.

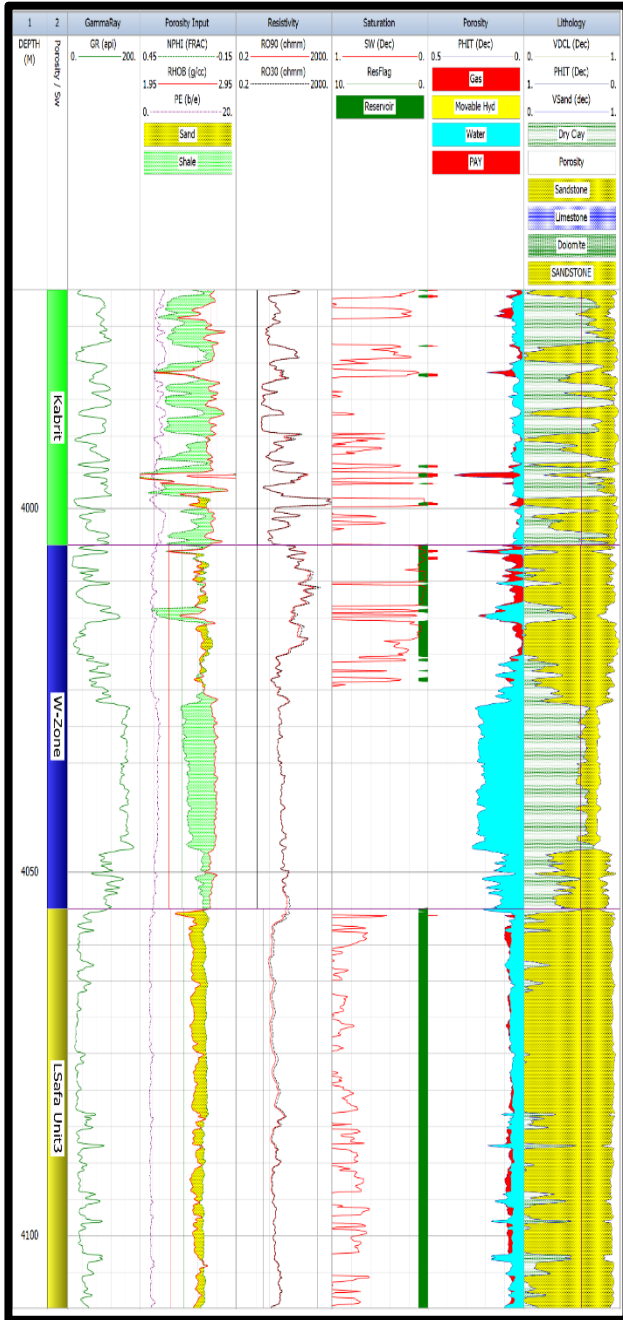


Fig. 7: Computed Petrophysical Interpretation (CPI) for OBA D-32 well.

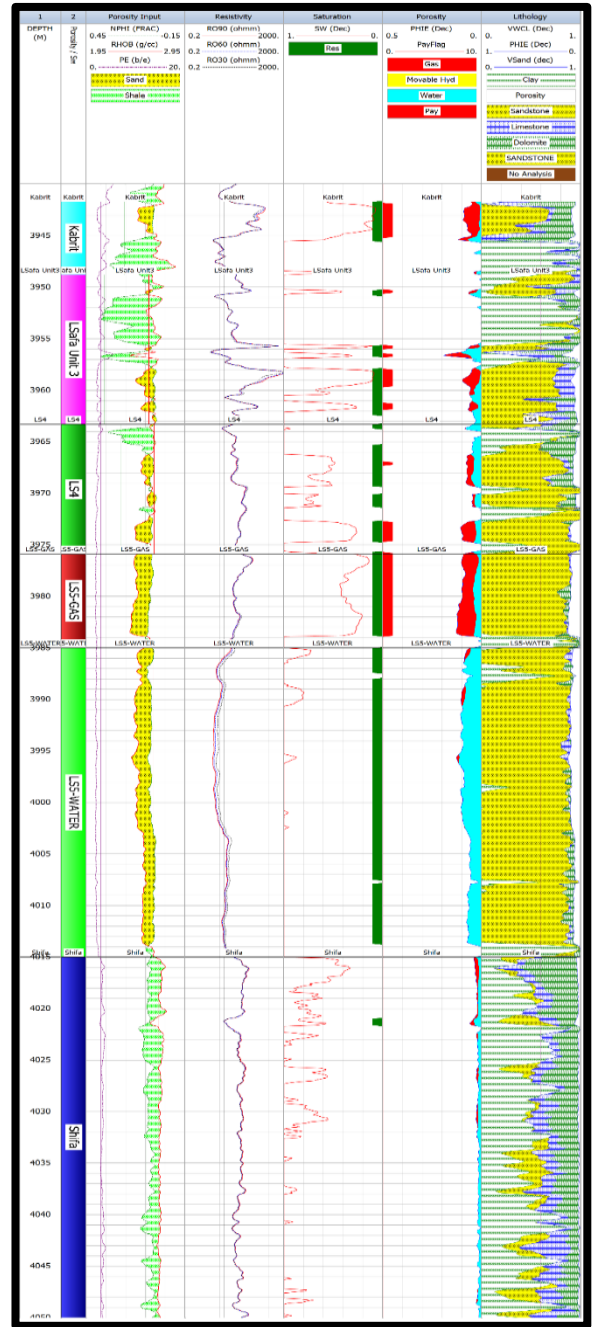


Fig. 8: Computed Petrophysical Interpretation (CPI) for OBA D-35 well.

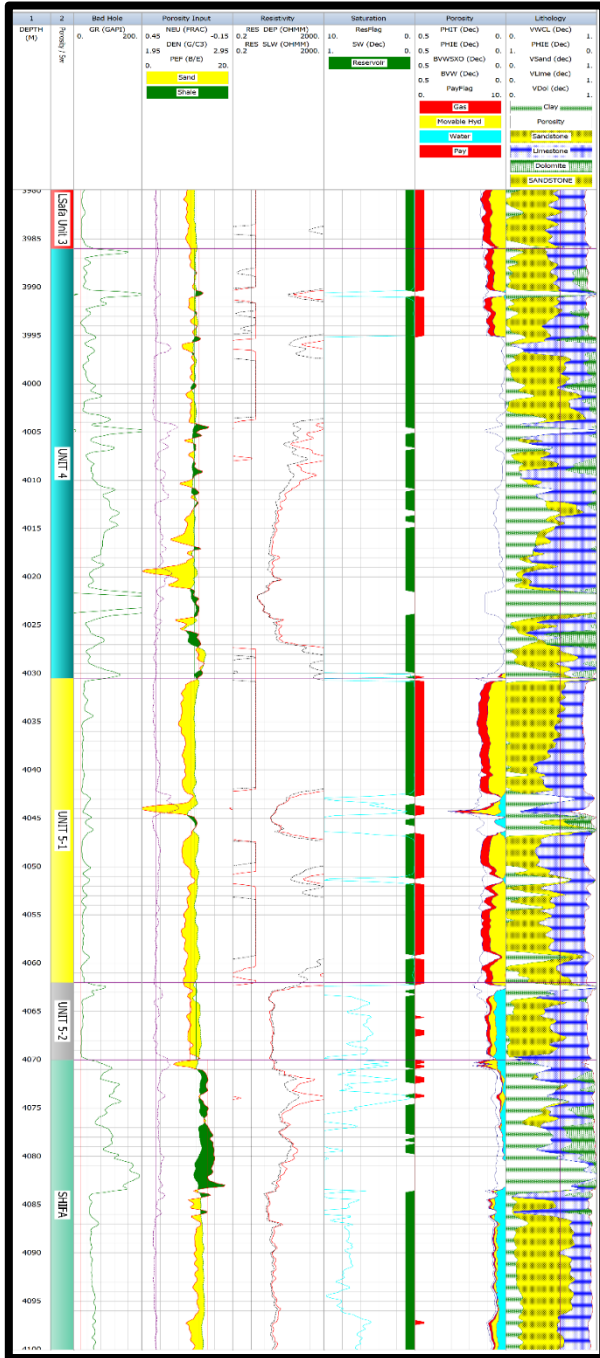


Fig. 9: Computed Petrophysical Interpretation (CPI) for D-19 well.

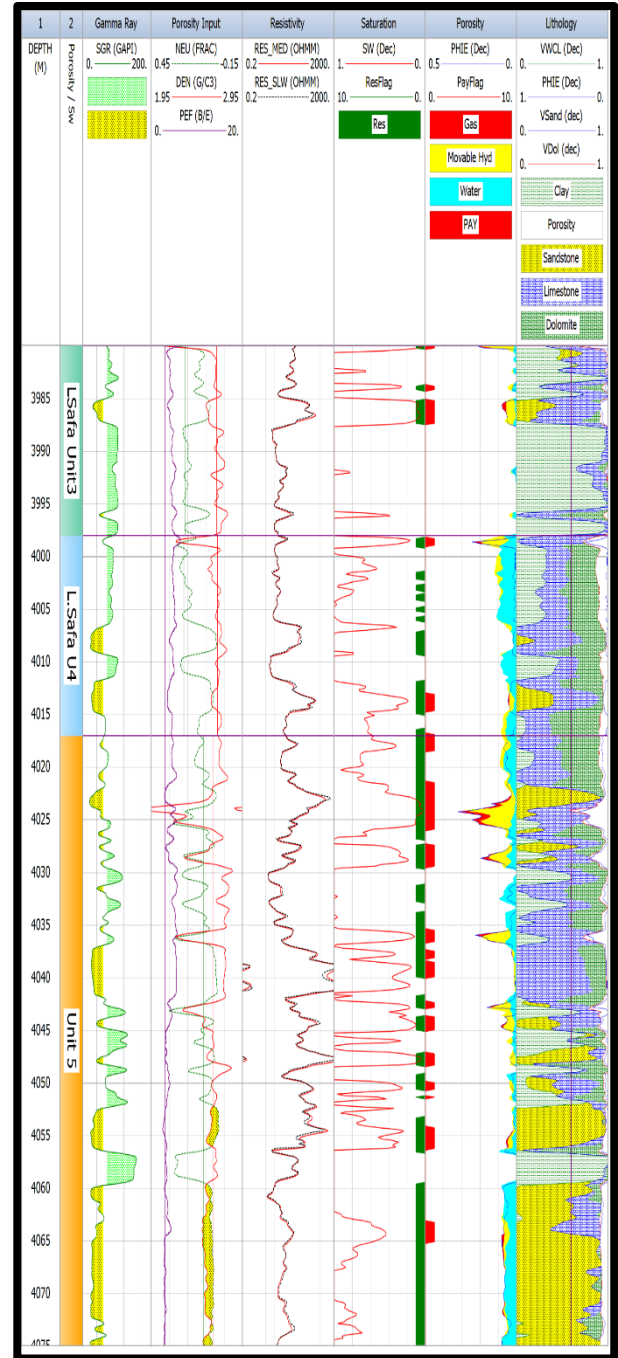


Fig. 10: Computed Petrophysical Interpretation (CPI) for D-15 well.

Apparent matrix which is a calculation of the properties of the solid fraction of a rock from the combination of two logs. For example, by combining the density and neutron porosity measurements, it is possible to compute an apparent matrix density and Density matrix, the density of a rock or mineral with no porosity, also known as matrix density, commonly in units of g/cm³.

Halliburton Apparent Matrix Vs Density Matrix cross plot is used, to identify the rock mineralogy. In the figures below (11, 12, 13 and 14) it is shown that the Lower Safa Units, which are the primary target gas-bearing reservoir, are made up of mainly clastic sediments, that contain substantial amount of hydrocarbons in D-15, D-19, OBA D-32 and OBA D-35 wells. This cross plot aided in the proper calculation of the reservoirs by adjusting quartz at the centre of points.

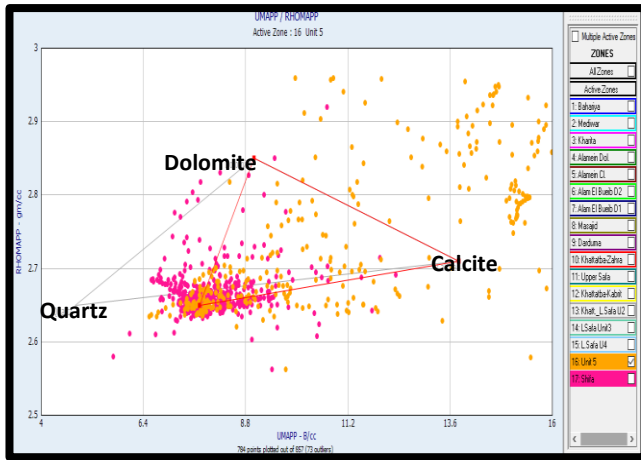


Fig. 11: D-15 well Halliburton Apparent Matrix Vs Density Matrix Cross Plot.

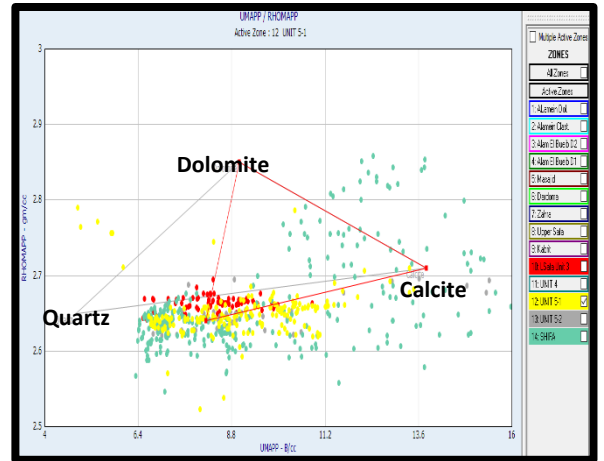


Fig. 12: D-19 well Halliburton Apparent Matrix Vs Density Matrix Cross Plot for well D15.

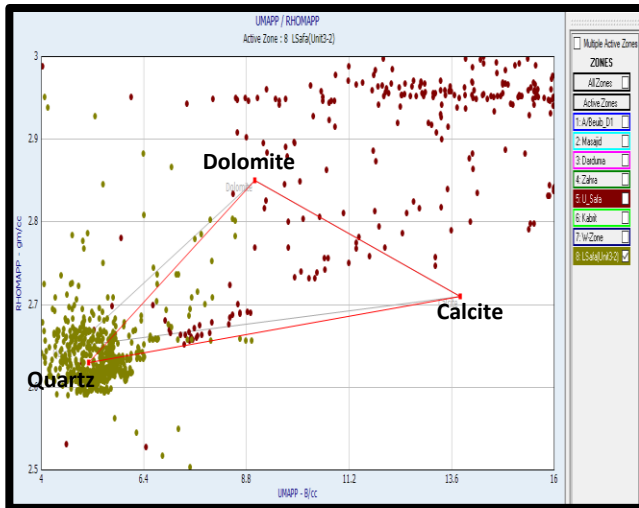


Fig. 13: OBA D-32 well Halliburton Apparent Matrix Vs Density Matrix Cross Plot.

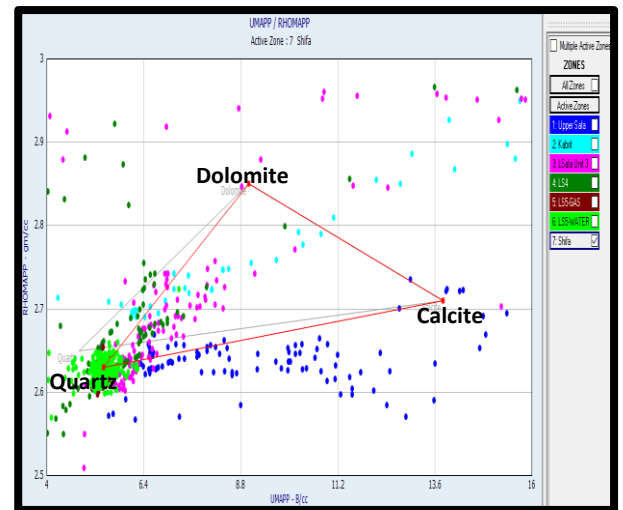


Fig. 14: OBA D-35 well Halliburton Apparent Matrix Vs Density Matrix Cross Plot.

Hydrocarbon saturation and the saturation-height factor is calculated using Archie's model. Archie's model uses density-porosity and deep resistivity as inputs, with the parameters M, N, and R_w , which are indicated for D-15, D-19, OBA D-32 and OBA D-35 wells in the tables below:

Table 1: D-15 well Safa Member Input values

Units	U.Safa	Unit 3-1	Unit 4	Unit 5-1&5-2
ρ_m	2.65	2.65	2.68	2.65
ρ_f	0.99	0.85	0.99	0.7&1.0
M	1.88	2.1	2.47	2.47
N	1.79	1.93	1.83	1.64
R_w	0.014	0.013	0.013	0.013

Table 2: D-19 well Safa Member Input values.

Units	U.Safa	Waste Unit 1&2	Unit 3	Unit 4	Unit 5
ρ_m	2.65	2.65	2.65	2.68	2.68
ρ_f	.99	.9	1.04	.99	.99
M	1.88	1.88	2	2	2
N	1.79	1.79	1.68	1.68	1.68
R_w	.013	.013	.013	.05	.05

Table 3: OBA D-32 well Safa Member Input values.

Units	Upper Safa	Lower Safa Unit-3	Lower Safa Unit-4	Lower Safa Unit5-Gas	Lower Safa Unit5-Gas
ρ_m	2.65	2.45	2.65	2.65	2.65
ρ_f	0.99	1	1	0.99	0.88
M	1.88	2.45	2.45	2.45	2.47
N	1.79	1.93	1.93	1.68	1.68
R_w	0.013	0.013	0.013	0.013	0.013

Table 4: OBA D-35 well Safa Member Input values

Units	Upper Safa	Waste Zone	Unit 3-2
ρ_m	2.65	2.65	2.65
ρ_f	0.99	1	1
M	1.88	1.88	2.45
N	1.79	1.79	1.93
R_w	0.013	0.013	0.04

D-15 Well

Table 5: D-15 well Safa Member Reservoir Parameters.

Zone Name	Gross Interval	Net Sand	Avg. Phi	N/G Ratio	Net Pay	Avg. Phi	Avg. Sw
	M	M	%	%	M	%	%
U. Safa	127	26	2.6	20.6	6.4	4.0	67.0
L. Safa Unit	31.5	5.9	6.0	18.9	3.83	7.7	33.5
Unit 2	9.5	5.08	10.2	53.5	5.08	10.2	9.0
Unit 3.1	18	2.98	6.4	16.5	2.98	6.4	9.9
Unit 4	19	9.94	3.2	52.3	2.63	7.1	50.4
Unit 5	58	44.44	6.1	76.6	19.9	7.5	53.0

The lithology of the Upper Safa reservoir in D-15 well consists of shale intercalated with sandstone and limestone streaks. While the Lower Safa reservoir consists mainly of sandstone with thin shale laminations and is divided to five units (Units 2, 3, 4 and 5) and the Net-Pay sand criteria depend on the cut-off parameters. $Sh > 50.0\%$ & $\Phi < 25.0\%$.

D-19 Well

The Upper Safa reservoir is composed mainly of shale and sandstone while the Lower Safa reservoir consists mainly of sandstone and some shale streaks. The Upper Safa reservoir is the secondary target of D19, which shows poor quality rock in the bottom part. The Lower Safa reservoir, which is the main target, comprises a high N/G sequence. The Lower Safa Member Unit 3 is mainly Sandstone. Unit 4 consists of silty-sand, with high shale content increasing with depth. Unit 5 is generally subdivided into two sub-units, Unit 5-1, shows the best sand quality encountered in this area and Unit 5-2 shows poor quality sand with low resistivity.

Table 6: D-19 well Safa Member Reservoir Parameters.

Zone Name	Gross Interval	Net Sand	Avg. Phi	N/G Ratio	Net Pay	Avg. Phi	Avg. Sw
	M	M	%	%	M	%	%
U.Safa	105	28.77	4.4	27.4	14.63	6.8	33.8
Lower Safa Unit 3-1	12	11.54	10.2	96.2	10.63	11.1	0.8
Unit 4	44.5	38.5	2.3	86.5	8.63	10.1	1.7
Unit 5-1	31.5	27.9	12.4	88.6	27.13	12.5	2.9
Unit 5-2	8	7.09	9.6	88.6	0.99	12.5	57.7

No porosity cut-off is used for the Net-Sand, while further cut-off for the Net-Pay determination, based on 50% <water saturation (S_w), has been applied. The value of 50% is based on the capillary pressure and saturation height function response. The base of Unit 5 sand is around 35mss above the free-water level (FWL=3875mss), assumed from D11 and D18 well, in which permeabilities below 0.1md correspond to water saturation above 50%. The following (Fig. 15) from BAPETCO internal reports shows the relationship between the height above FWL, permeability and saturation.

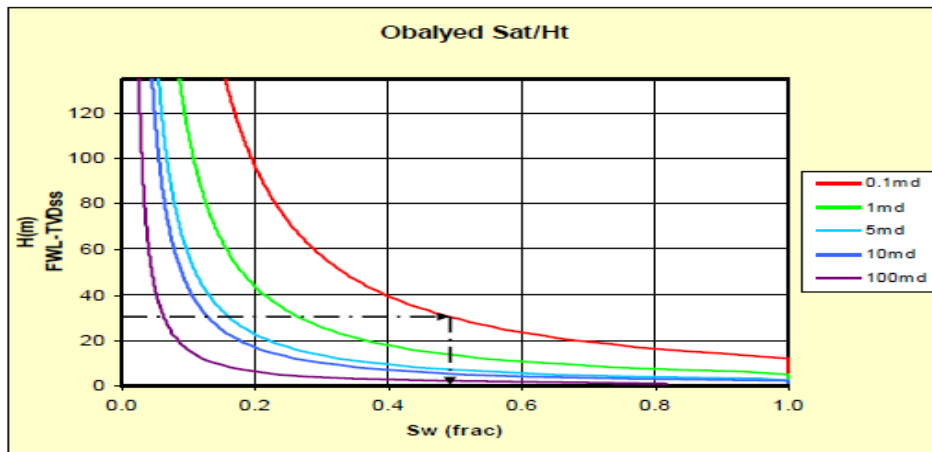


Fig. 15: Relationship between the height above FWL, permeability and saturation.

Lithology & Facies Identification:

The main clay minerals in the Lower Safa reservoir are kaolinite and illite. The Schlumberger Potassium/Thorium crossplot below shows that the clay type to be kaolinite in Unit 3 of D19 well, and that, the Unit3 in D19 well is cleaner. Similarly, Unit 5-1 in D19 well appears clean with dominantly kaolinite clays, see (Fig. 16). Illite appears in Unit 5-2 of D19 well, which results in the severe decrease in permeability observed in this sub-unit.

OBA D-32 Well

The objective of this well is to test the presence of economic volumes of hydrocarbons in the Middle Jurassic Lower Safa sandstone reservoirs, contained in El-Obaiyed NW structure. The Lower Safa sands hopefully are predicted to be gas/condensate reservoirs. The Upper Safa reservoir consists mainly of shale and poor sand streaks, while the Lower Safa reservoir consists of sandstone with some shale streaks.

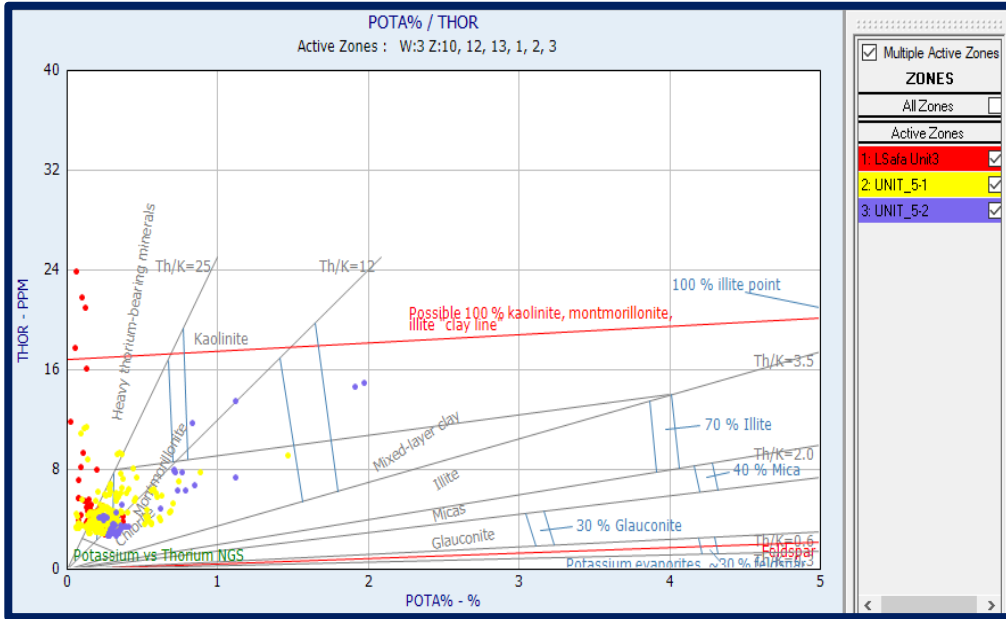


Fig. 16: Schlumberger Potassium-Thorium Cross Plot for D19 well.

Table 7: OBA D-32 well Safa Member Reservoir Parameters.

Zone Name	Gross Interval	Net Sand	Avg. Phi	N/G Ratio	Avg. Sw
	M	M	%	%	%
Upper Safa	128.1	4.1	7.6	3.2	9.9
Waste Zone	50	14.2	5.1	28.5	12.5
Lower Safa (Unit 3-2)	82	72.2	6	88.1	85.7

OBA D-35 Well

From well logs, we can identify the Upper Safa and Lower Safa (Unit-4), as gas-bearing reservoirs. The top part of Lower Safa Member (Unit-5) is a gas-bearing reservoir, as well.

The Upper Safa and Kabrit rock units consist of sandstone and Shale. The Lower Safa consists mainly of sandstone with some streaks of shale. The Lower Safa member can be further divided to four units. The first three units in the Lower Safa hold a fair percentage of hydrocarbon saturation, while the L.S Unit 5-Water is water-bearing.

Table 8: OBA D-35 well Reservoir Parameters.

Zone Name	Gross Interval	Net Sand	Avg. Phi	N/G Ratio	Net Pay	Avg. Sw
	M	M	%	%	M	%
Upper Safa	10	3	6.4	30	3	19.8
Lower Safa Unit-3	14.5	6.35	6.9	43.8	3.2	49.7
Lower Safa Unit-4	12.6	8.2	7.0	65.1	2.35	56.1
Lower Safa Unit5-Gas	9.1	8	10.5	87.9	7.95	29.9
Lower Safa Unit5-Water	30	28	8.3	93.2	---	97.5

4.3 Structural Well Correlation

Correlation of multi-well log is constructed for (D-15, D-19, OBA D-32, OBA D-35) wells following the petrophysical and lithologic evaluation of the main productive zones. This correlation chart is concentrated mainly in the Lower Safa reservoir. This has the advantage of emulating the change in thickness and connectivity of the area productive zones for further understanding of the existing structure. (Fig. 17) shows the correlation between the previously mentioned wells, illustrating the variance from north to south.

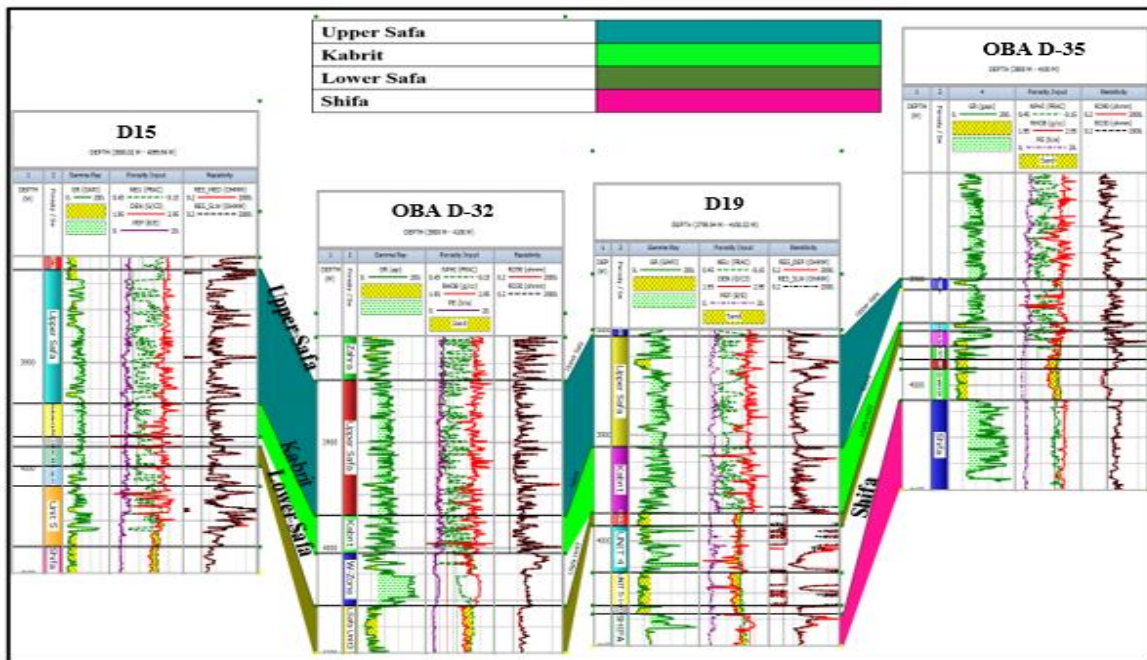


Fig. 17: Structural Well Correlation between El-Obaiyed Field wells (D-15, D19, D-32, D-35).

4.4 Stratigraphic Well Correlation

The lower Safa reservoir is partitioned into several sand units, according to the gamma-ray and neutron-density log curves in D-15, D-19, OBA D-32 and OBA D-35 wells. The reservoir sand units are then correlated stratigraphically along the logs, to identify the continuity of the reservoir across the studied wells, which are found not connected, as they lie in the different compartments of the area (Fig. 18).

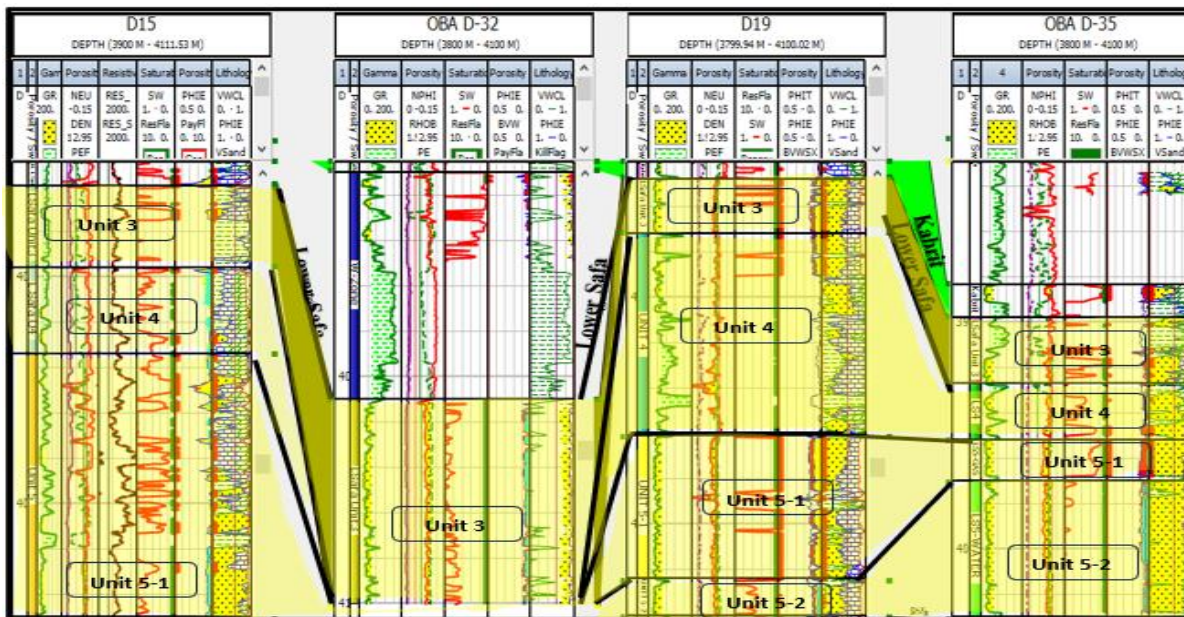


Fig. 18: Stratigraphic Well Correlation between El-Obaiyed Field wells (D-15, D-19, D-32, D-35).

5. Petrophysical Results Interpretation

In this section of the paper, the geophysical and geological outcomes acquired will be combined, to delineate and annotate the structures, hydrocarbon potentialities, distribution of the Upper and Lower Safa reservoirs in Khatatba Formation, El-Obaiyed Gas Field, Matruh area. The previous steps would alleviate the opportunity of uncommercial development and aid in the risk assessment. The petrophysical and geological results obtained from the wireline log evaluation data in El-Obaiyed Field wells are used, to evaluate the petrophysical characteristics, thickness distributions and the depositional environments of the potential formations concentrated mainly in Lower Safa Member (primary reservoir) and Upper Safa Member (secondary reservoir).

5.1 Pressure Performance

By assessing the pressure data of the potential zones in Khatatba Formation, essentially in the Lower Safa Member Unit 5-Gas which showed good pay sand, pressure points in D-19 and OBA D-35 wells are 2930 Psi and 4500 psi respectively. The fluid type wasn't confirmed in OBA D-35 well due to the low mobility and depletion at 1500 psi in the rich gas-zone. Unit-4 indicated un-stabilized and poor-quality rock in D-19 well, where it shows no valid gradient and depletion at 1500 psi in OBA D-35 well. Unit-3 returned with 4025 psi, with an overestimation of 1000 psi in D-19 well. Well D-15, showed only valid points with Unit-1 in the Lower Safa, which was tight sand. The Upper Safa Member showed virgin pressure in D19 well and was over-pressurized by 1500 psi in OBA D-35 well.

The Multi-well correlation constructed between the wells (D-15, D-19, OBA D-32, OBA D-35) zones and reservoirs revealed thinning in thickness in the Lower Safa Member southwards, due to the

change in depositional environment, which is located at the higher part of Matruh basin. Whereas northward of the Lower Safa Member is thicker towards the deep center of the basin. Corresponding to the results with the pressure data, it is therefore more ideal that, the sand reservoir zones are not connected.

Moreover, each well has its own GDT (Gas-Down-To) value in the Lower Safa Member, where D-15 well shows GDT @3875 TVDSS, 3821 TVDSS in D-19 well and 3748.5 TVDSS in OBA D-35 well, while OBA-32 well was wholly water-bearing. Thus, the pressure points of the potential zones discussed data and the incompatible GDT values confirm that the D19, D15 and OBA D35 wells lie in different zones, where each well has its own characteristics and properties, that is individual to this specific area.

5.2 Sedimentary Facies

The overall facies of the Lower Safa Member comprise tidal dominated and fluvial dominated deposits (Internal Report). This formation is made up of sand-shale intercalations, with several types of sands. The essence of the facies change in the sub-units is the content of clay mineral, particularly illite. The predominant clay mineral in the Lower Safa Member is kaolinite, which is dominated in unit 5-Gas and unit-3 in D-19 well and the presence of both Illite and Kaolinite at the bottom of unit-5 (water-zone), explaining the substantial decrease in permeability.

The Lower Safa Member unit-5 is made up of well sorted, and coarse-grained sand, which also shows a cylindrical shape response in the Gamma Ray log without any sedimentary structure, due to its deposition in an alluvial fan or braided channel. Units 2 to 4 in the Lower Safa Member are tidal dominated sands, which are characterized by varying sizes sand finning upward, moderately to poorly sorted, as indicated by the bell shape response in the Gamma- Ray log. These variations in the formation units and change in the lithology have a huge effect on the porosity and permeability as we have encountered in D-19 well and on the sealing capacity and its presence, as was revealed in the Upper Safa Member D-15 well. The occurrence of lithologic lateral variations might have been the obstruction to the migration of hydrocarbons to the reservoir rocks of OBA D-32 non-producing well.

6. SUMMARY AND CONCLUSIONS

El-Obaiyed Gas Field is located at the western flank of Matruh Basin, north Western Desert of Egypt, some 50 km south of the Mediterranean coast and about 450 km WNW of Cairo. It produces gas from the Khatatba Formation (Middle Jurassic). The petrophysical evaluation of the Lower Safa Member primary reservoir showed thinning to the south west and noticeable thickening to the north eastern direction, towards the depocenter of Matruh Basin. This is due to the Mesozoic (Tethyan) rifting across the north Western Desert. The Lower Safa Member was segmented into five units in this study, based on the gamma-ray and neutron-density logs, which are composed of sand and shale intercalations. The neutron-density log response identified that, gas is the hydrocarbon fluid in the Lower and Upper Safa members. The Lower Safa Member shows that, the optimum net-pay sand zones are in units 3 and 5. The Sand units are characterized by higher effective porosity and permeability values.

Furthermore, the gamma-ray log response shows a cylindrical shape in unit 5, which is related to the deposition in an alluvial fan or braided channel. Meanwhile, a bell shaped gamma-ray response in units 2 to 4 is attributed to the deposition in a tidal channel environment. The pressure data showed that, each well lies in a different area, as the Lower Safa pressure readings are not homogenous with an individual Gas-Down-To value for the producing wells.

The highest relief is located at the center of the basin, which would be the best position for further developments in the field. The facies identification from the available wells and gamma response represents a braided or alluvial fan and tidal dominated depositional environment. This is due to the variation in lithology and clay minerals affecting the porosity, permeability values and the sealing capacity in the Lower Safa Member units.

The producing D-15, D-19 and OBA D-35 wells are identified to lie in the different zones shown by the different GDT values and pressure point readings. OBA D-32 well is identified as wholly water-bearing, due to the likelihood of secondary migration and the well-being in a varying zone, showing no continuity of the sand reservoir.

The impact of rock physics is a vital technique, that can be used for the evaluation of hydrocarbon types and their occurrences. All the petrophysical parameters can affect the reservoir potentiality and this includes the type and quality of lithology in the reservoir, porosity and permeability, which help in indicating the free movability of the fluids. The thickness and type of sealing preserve the fluids from escaping. Also, the correlation to evaluate the connection between the wells in the field, aided the conclusion of the individuality of each well and the presence of several compartments in the field.

Declaration of interest

The corresponding author discloses any potential competing or non-financial interests on behalf of all authors of the work.

6. References

- Archie, C.E. (1942), The electrical resistivity logs as an aid in determining some reservoir characteristics, Transactions of the AIME, Vol.146, pp.54-62.
- Asquith, B. G. (1990), Log Evaluation of Shaly Sandstone Reservoirs: A Practical Guide, The American Association of Petroleum Geologists.
- Ayouty, M.K., El Homossany, A. A., Abdel Karim, H. I., and Rateb R. (1996), Oil and Gas Exploration in Egypt (a historical review 886-1996). The 13th Petroleum Conference, Cairo, pp. 53.
- Avseth, P., Jørstad, A., van Wijngaarden, A.-J., and Mavko, G., et al (2009): Rock physics estimation of cement volume, sorting, and netto gross in North Sea sandstones: The Leading Edge, 28, no. 1, 98– 108.
- Abdel-Fattah, M. I. (2015), Impact of depositional environment on petrophysical reservoir characteristics in Obaiyed Field, Western Desert, Egypt, Saudi Society for Geosciences.
- Ahmed, S., Elwegaa, K., Htawish, M., Alhaj Haiat (2019) Determination of the Oil Initial in Place, Reserves, and Production Performance of the Safsaf C Oil Reservoir.

Attiya, A., S., Kassab, M., A., Salem, T., M., Abbas, Al E. (2023), Source rock evaluation and burial history modelling of the Middle Jurassic Khatatba Formation in the West Kanayes Concession of Matruh Basin, North-Western Desert, Egypt, Khaldia Petroleum Company, Egyptian Petroleum Research Institute, Faculty of Petroleum and Mining Engineering – Suez University.

Bosworth, William & Tari, Gabor. (2021). Hydrocarbon accumulation in basins with multiple phases of extension and inversion: examples from the Western Desert (Egypt) and the Western Black Sea. *Solid Earth*. 11. 1-20. 10.5194/se-12-59-2021.

Egyptian General Petroleum Corporation (EGPC), (1992): Western Desert, oil and gasfields, a comprehensive overview. EGPC 11th Exploration and Production Conference, Cairo, Egypt, 431p.

Farag, M. I. A. (2010), Geophysical Reservoir Evaluation of Obaiyed Field, Western Desert, Egypt, Technical University, Berlin, pp. 11-15, 31, 51.

Ghanima, A., El-Bendary, A., Taha, A., Fara, Y., Gamal, A., Abbas, S., A., Samantray, A., Ibrahim, H. (2015), An Integrated Petrophysical, Geochemical and Operational Approach to Identify Unconventional Resource, Case Study, Obayed Field, Western Desert, Egypt, Society of Petroleum Engineers (SPE) – 175744-MS.

Gomaa, M., M. 2017, Petrophysical Seismic Study of the Jurassic Sandstone Reservoirs: El-Obaiyed Field, Western Desert, Egypt, Ain Shams University, Egypt.

Hamimi, Z., El-Barkooky, A., Frias, J. M., Fritz, H., Abd El-Rahman, Y. (2020), *The Geology of Egypt*, Springer, pp. 254-258.

Mohamed, H.S., Abdel Zaher, M., Senosy, M.M. et al. Correlation of Aerogravity and BHT Data to Develop a Geothermal Gradient Map of the Northern Western Desert of Egypt using an Artificial Neural Network. *Pure Appl. Geophys.* 172, 1585–1597 (2015).

Said, R. (1962): *The geology of Egypt*. Elsevier Publishing Co., Amsterdam, New York, 337 p. Schlumberger (1984), *Geology of Egypt*, Well Evaluation Conference, Egypt, pp.1-34.

Saad, (2010): Lower Safa sedimentological study, new insights in the reservoir quality distribution of the Obaiyed field, Western Desert, Egypt, Society of Petroleum Engineers.

Younes, M. A. (2012), *Hydrocarbon Potentials in the Northern Western Desert of Egypt*, Alexandria University, Egypt, pp. 26-32.